Organ doses for monkey anatomy models with different postures exposed to external photons

Jae Won Jung[1], Daniel D. Lee[2], Ae-Kyung Lee[3], Hyungdo Choi[3]

[1]Department of Radiation Oncology, East Carolina University, Greenville, NC, 27858, USA

[2]Thomas S. Wootton High School, Rockville, MD, 20850, USA

[3]Radio & Satellite Research Division, Electronics and Telecommunications Research Institute, Daejeo 34129, South Korea

Submitted to Radiation Protection Dosimetry

Abstract

Background: Understanding how external radiation from nuclear accidents or radiological attacks affects internal human anatomy is essential to accurately assess health risks and develop effective treatments. In the current study, we used the Monte Carlo radiation transport methods to create a library of organ dose conversion coefficients for an anatomical monkey model in various postures exposed to six different irradiation geometries.

Methods: We adopted previously published anatomical monkey models with three different postures: crawling, squatting, and standing. Radiation doses to a total of 39 organs and tissues were calculated using a general-purpose Monte Carlo radiation transport code, MCNP6, for 33 mono-energetic photon fields ranging from 0.01 to 20 MeV with six different irradiation geometries: antero-posterior (AP), postero-anterior (PA), left lateral (LLAT), right lateral (RLAT), rotational (ROT), and isotropic (ISO).

Results: We found that the dose conversion coefficients derived from the standing posture may overestimate organ dose by up to 13-fold compared to the crawling position (e.g., large intestine in AP irradiation geometry). Irradiation geometry has the most substantial impact on organ doses in the crawling posture compared to squatting and standing postures. Average coefficients of variation over different organs were 51% in crawling posture compared to 16% and 17% for standing and squatting postures, respectively.

Conclusion: In the present research, we employed the Monte Carlo radiation transport techniques to develop a library of organ dose conversion coefficients for an anatomical monkey model considering various postures and six distinct irradiation geometries. We found that the existing dose conversion coefficients for the standing posture may substantially overestimate organ doses for monkeys in more natural postures. Our data should be useful for understanding the impact of radiation events to human anatomy by evaluating the impact on monkey's anatomy as a surrogate.

Introduction

Monkeys have played a crucial role in understanding the impact of acute radiation exposure on human health, particularly in the context of radiation treatment[1–5] or a mass casualty incident such as nuclear accidents[6,7] and radiological attacks by terrorists[8–11]. Due to their genetic and physiological similarities to humans, non-human primates have been extensively studied to model the effects of high-dose radiation exposure. Research involving monkeys has provided valuable insights into how radiation affects organ systems, immune response, and overall survival. These studies have informed medical countermeasures and treatment protocols for radiation sickness in humans, enhancing preparedness for potential nuclear incidents and radiological emergencies.

Understanding how external radiation from nuclear accidents or radiological attacks affects internal human anatomy is essential to accurately assess health risks and develop effective treatments. In this context, Japanese researchers investigated the impact of the Fukushima Daiichi nuclear accident on wild Japanese monkeys living near the site to assess radiation exposure. While this study provided valuable insights into the biological effects of radiation, it did not consider posture-related differences in monkey anatomy which could affect the distribution of radiation doses to internal organs and tissues. Given that radiation experiments on monkeys are both labor-intensive and costly, computer simulations of radiation behavior and computerized anatomical models of monkeys could offer a more efficient and effective method to evaluate the radiation burden on monkey anatomy. More recently, Chung et al.[12] introduced a computational model of a monkey and calculated organ dose conversion coefficients—organ dose (Gy) normalized to air kerma (Gy)—through simulations for external photon exposure[13]. Air kerma, which is commonly measured or available during most radiation events, allows these coefficients to be converted into absolute organ doses. However, organ doses can vary significantly depending on the monkey's posture and there is limited data on this variation.

In the current study, we used the Monte Carlo radiation transport methods to create a library of organ dose conversion coefficients for an anatomical monkey model in various postures exposed to six different irradiation geometries. We then compared the results to assess how different postures affect internal organ doses.

Material and method

We adopted previously published anatomical monkey models with three different postures: crawling, squatting, and standing. Radiation doses to a total of 39 organs and tissues were calculated using a general-purpose Monte Carlo radiation transport code, MCNP6, for 33 mono-energetic photon fields ranging from 0.01 to 20 MeV with six different irradiation geometries:

antero-posterior (AP), postero-anterior (PA), left lateral (LLAT), right lateral (RLAT), rotational (ROT), and isotropic (ISO).

Computational monkey models

We adopted a computational monkey model in standing posture developed by Chung et al.[12,14] and later modified into two different postures[15]. The original model was developed through the Visible Monkey project conducted at the Electronics and Telecommunications Research Institute in South Korea using sectioned photographs of the whole-body female rhesus monkey. The monkey was frozen while the monkey was lying on the table so the actual posture would be "lying" but we used the term "standing" equivalent to the human posture. A total of 177 anatomical structures were segmented by anatomists and the structures in mesh format were converted into voxel format, which is compatible with the Monte Carlo radiation transport code. Figure 1 illustrates the monkey model in a standing position, showcasing both the front and rear perspectives where major organs and tissues are indicated. Figures 2 and 3 show the top, frontal, and lateral views of the monkey models in crawling and squatting postures, respectively.

Monte Carlo radiation transport

We calculated the absorbed dose conversion coefficients (Gy/Gy) for major organs in computational monkey models using Monte Carlo radiation transport techniques. The dose calculations were performed with the general-purpose Monte Carlo transport code MCNP6(3). Although the mesh format is compatible with MCNP6, we chose the voxel format because the mesh format was expected to provide no additional benefits. The three models were voxelized into 1 x 1 x 1 mm3 resolution and the final voxel matrix size was 291 x 374 x 629, 199 x 355 x 500, and 229 x 148 x 757 for the crawling, squatting, and standing monkey models, respectively. The heights of the three models were about 63 (crawling), 50 (squatting), and 76 cm (standing). The voxel-format models of monkeys in crawling, squatting, and standing positions were converted to a lattice file format compatible with MCNP6. For the dose to small organs and thin tissues (e.g., skin) to be accurate, we employed the *F8 tally to fully track secondary electrons instead of *F6 tally, where kerma approximation is adopted. MCNP6 was running on a Mac Studio equipped with Apple M2 Ultra CPU 24 cores with the memory of 128 GB.

Organ dose calculations

Radiation doses to a total of 39 organs and tissues were calculated using the Monte Carlo simulation method (Table 1). The three monkey models were exposed to broad parallel idealized photon beam fields in six different irradiation geometries: AP, PA, LLAT, RLAT, ROT, and ISO, which are defined in ICRP Publication 116[16]. The frontal direction was aligned with the orientation of the monkey's eyes. Mono-energetic photon beams were created in broad parallel fields covering the

whole body of the monkey models with the energy ranging from 0.01 to 20 MeV. Total calculation for all monkey models, irradiation geometries, and energy bins took about a week including spot checking and rerunning some inputs with errors. The resulting dose per photon (Gy/photon) was then normalized to the fluence-to-air kerma conversion coefficients reported in ICRP Publication 116[16]. Dose conversion coefficients for major organs were analyzed to evaluate the impact of irradiation geometry and postures on internal organ dose by different postures.

Results

Organ dose conversion coefficient library

We calculated a library of organ dose conversion coefficients (Gy/Gy), organ absorbed dose (Gy) normalized to air kerma (Gy), for a total of 39 organs and tissues for the monkey models in crawling, squatting, and standing postures exposed in AP, PA, LLAT, RLAT, ROT, and ISO geometries. The full library is tabulated in an Excel file and provided as a supplementary material.

Impact of posture on organ dose

All major organs (stomach, liver, and large intestine) of the monkey model in standing posture received the greatest dose in AP irradiation geometry (Figure 4A-4C), which would be the most common exposure scenario in radiation accident or terrorists' attack. Only the lungs in standing posture received a slightly smaller dose than that in squatting posture (Figure 4D). The organs of the monkey model in crawling posture always received the smallest dose compared to other two postures in AP irradiation geometry. At the photon energy of 0.08 MeV, where the standing posture shows the maximum values, the stomach, liver, large intestine, and lung of the monkey in standing posture received 2.9-, 2.3-, 12.6-, and 2.4-fold, respectively, greater dose compared to those of the monkey in crawling posture. Compared to the squat posture at 0.08 MeV, both stomach and large intestine in standing posture still received greater dose by 1.2-fold than those in squatting posture but liver and lung doses were similar.

All organs of the monkey in crawling posture received the greatest dose in RLAT irradiation geometry compared to the squatting and standing posture (Figure 5). Stomach, liver, large intestine, and lung received greater dose by 1.01, 1.04, 1.03, and 1.17-fold compared to the standing posture at 0.08 MeV. All major organs in the squatting posture always received the smallest dose among the three postures. Stomach, liver, large intestine, and lung in squatting posture received 70%, 81%, 99%, and 89% of the doses in standing posture.

Impact of irradiation geometry on organ dose

Irradiation geometry has the most substantial impact on organ doses in crawling posture (Figure 6) compared to squatting (Figure 7) and standing (Figure 8) postures. For the crawling posture, the coefficient of variation (COV) (standard deviation divided by average) across the different irradiation geometries in stomach, liver, large intestine, and lung doses was 43%, 59%, 50%, and 53%, respectively, for a 0.08 MeV energy bin. The maximum dose at 0.08 MeV was 3.9-, 12.2-, 11.2-, and 10.5-fold greater than the minimum dose for stomach, liver, large intestine, and lung, respectively, across different irradiation geometries.

In contrast to a crawling posture, COV at 0.08 MeV across different irradiation geometries was 18%, 22%, 11%, and 17% in squatting posture (Figure 7) and 14%, 23%, 15%, and 12% in standing posture (Figure 8) for stomach, liver, large intestine, and lung, respectively. The ratio of maximum to minimum dose was 1.67, 1.92, 1.35, and 1.53 in squatting posture and 1.43, 2.06, 1.52, and 1.33 in standing posture for stomach, liver, large intestine, and lung, respectively.

Discussion

We first calculated a comprehensive library of organ-specific dose conversion coefficients for three monkey models in crawling, squatting, and standing postures exposed to a variety of external photon irradiation geometries. Compared to the existing data calculated for the standing posture[13], the crawling and squatting postures are more natural for living monkeys exposed to radiation events. Our simulation scenarios also include ISO irradiation geometry, where radiation enters monkey's anatomy from all surrounding directions. This geometry along with AP would be the most plausible exposure scenarios in radiation accidents compared to other geometries such as PA, LLAT, and RLAT.

We found that the dose conversion coefficients derived from the standing posture may overestimate organ dose by up to 13-fold compared to the crawling position (e.g., large intestine in AP irradiation geometry). Overestimation was not significant when dose coefficients in standing posture was applied to squatting posture. Dose coefficients in standing posture showed a relatively small difference compared to other natural postures in RLAT geometry, where the position of arms provided shielding to internal organs.

Irradiation geometry has the most substantial impact on organ doses in the crawling posture compared to squatting and standing postures. Average coefficients of variation over different organs were 51% in crawling posture compared to 16% and 17% for standing and squatting postures, respectively.

We are aware of several limitations of the current study. Our result is based on a single monkey model and the results may vary by different monkeys depending on the anatomical variation and

postures. Dose calculation for some critical tissues in case of human anatomy such as red bone marrow was not attempted due to lack of red marrow distribution in monkeys. This will be explored more in the future by collecting data from the literature.

Conclusion

In the present research, we employed the Monte Carlo radiation transport techniques to develop a library of organ dose conversion coefficients for an anatomical monkey model considering various postures and six distinct irradiation geometries. We found that the existing dose conversion coefficients for the standing posture may substantially overestimate organ doses for monkeys in more natural postures. Our data should be useful for understanding the impact of radiation events to human anatomy by evaluating the impact on monkey's anatomy as a surrogate.

Acknowledgement

ETRI will add

References

1. Rohrer, M. D., Kim, Y. and Fayos, J. V. *The effect of cobalt-60 irradiation on monkey mandibles*, Oral Surg Oral Med Oral Pathol **48**(5), 424–440 (1979).

2. Cui, W., Bennett, A. W., Zhang, P., Barrow, K. R., Kearney, S. R., Hankey, K. G., Taylor-Howell, C., Gibbs, A. M., Smith, C. P. and MacVittie, T. J. *A non-human primate model of radiation-induced cachexia*, Sci Rep **6**(1), 23612 (2016).

3. Wood, D. H. *Long-Term Mortality and Cancer Risk in Irradiated Rhesus Monkeys*, Radiation Research **126**(2), 132–140 (1991).

4. Lett, J. T., Lee, A. C. and Cox, A. B. *Late Cataractogenesis in Rhesus Monkeys Irradiated with Protons and Radiogenic Cataract in Other Species*, Radiation Research **126**(2), 147–156 (1991).

5. Schultheiss, T. E., Stephens, L. C., Jiang, G.-L., Kian Ang, K. and Peters, L. J. *Radiation myelopathy in primates treated with conventional fractionation*, International Journal of Radiation Oncology*Biology*Physics **19**(4), 935–940 (1990).

6. Ochiai, K., Hayama, S., Nakiri, S., Nakanishi, S., Ishii, N., Uno, T., Kato, T., Konno, F., Kawamoto, Y., Tsuchida, S. and Omi, T. *Low blood cell counts in wild Japanese monkeys after the Fukushima Daiichi nuclear disaster,* Sci Rep **4**(1), 5793 (2014).

7. Hayama, S., Nakanishi, S., Tanaka, A., Konno, F., Kawamoto, Y. and Omi, T. *Influence of radiation exposure to delayed fetal growth in wild Japanese monkeys after the Fukushima accident*, Front. Vet. Sci. **10** (2023).

8. Hérodin, F., Richard, S., Grenier, N., Arvers, P., Gérome, P., Baugé, S., Denis, J., Chaussard, H., Gouard, S., Mayol, J.-F., Agay, D. and Drouet, M. *Assessment of total- and partial-body irradiation in a baboon model: preliminary results of a kinetic study including clinical, physical, and biological parameters*, Health Phys **103**(2), 143–149 (2012).

9. Ossetrova, N. I., Sandgren, D. J. and Blakely, W. F. *Protein biomarkers for enhancement of radiation dose and injury assessment in nonhuman primate total-body irradiation model*, Radiation Protection Dosimetry **159**(1–4), 61–76 (2014).

10. Valente, M., Denis, J., Grenier, N., Arvers, P., Foucher, B., Desangles, F., Martigne, P., Chaussard, H., Drouet, M., Abend, M. and Hérodin, F. *Revisiting Biomarkers of Total-Body and Partial-Body Exposure in a Baboon Model of Irradiation*, PLoS One **10**(7), e0132194 (2015).

11. Bolduc, D. L., Villa, V., Sandgren, D. J., Ledney, G. D., Blakely, W. F. and Bünger, R. *Application of Multivariate Modeling for Radiation Injury Assessment: A Proof of Concept*, Computational and Mathematical Methods in Medicine **2014**, 1–17 (2014).

12. Chung, B. S., Jeon, C.-Y., Huh, J.-W., Jeong, K.-J., Har, D., Kwack, K.-S. and Park, J. S. *Rise of the Visible Monkey: Sectioned Images of Rhesus Monkey*, Journal of Korean Medical Science **34**(8) (2019).

13. Lee, S. M., Choi, C., Shin, B., Lee, Y., Choi, J. W., Cheon, B.-W., Min, C. H., Chung, B. S., Choi, H. J. and Yeom, Y. S. *Implementation of Visible monkey into general-purpose Monte Carlo codes: MCNP, PHITS, and Geant4*, Nuclear Engineering and Technology **55**(11), 4019–4025 (2023).

14. Kim, C. Y., Lee, A.-K., Choi, H.-D. and Park, J. S. *Dawn of the Visible Monkey: Segmentation of the Rhesus Monkey for 2D and 3D Applications*, Journal of Korean Medical Science **35**(15) (2020).

15. Kim, C. Y., Lee, A.-K., Choi, H.-D. and Park, J. S. *Posture-Transformed Monkey Phantoms Developed from a Visible Monkey*, 10, Applied Sciences **11**(10), 4430 (2021).

16. ICRP. *Conversion Coefficients for Radiological Protection Quantities for External Radiation Exposures*, ICRP Publication 116, Ann. ICRP **40**(2–5), 1–258 (2010).

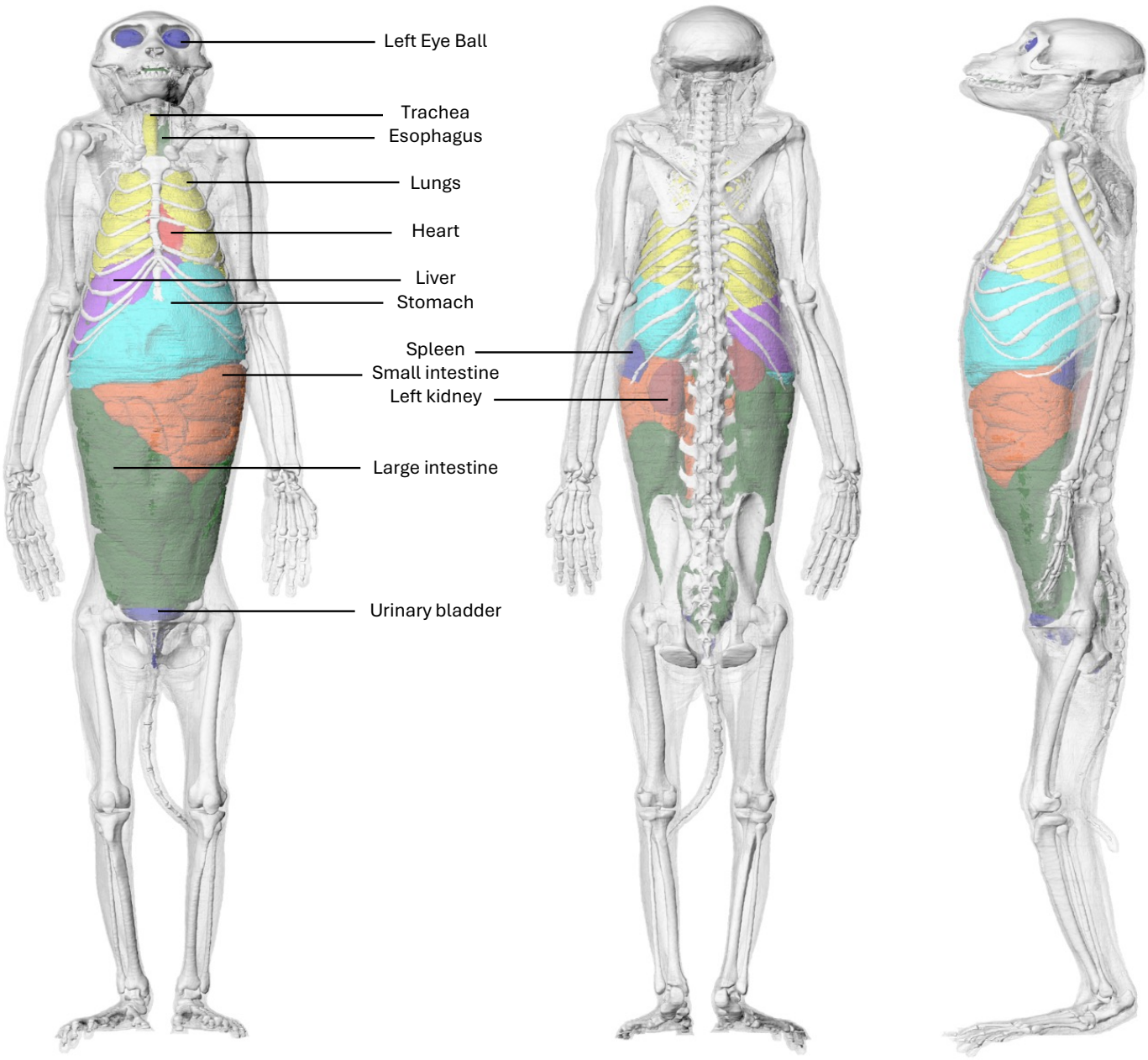

Figure 1. Frontal (left), rear (middle), and lateral (right) views of the monkey model in standing posture. Major organs indicated.

(a) top

(b) frontal

(c) left lateral

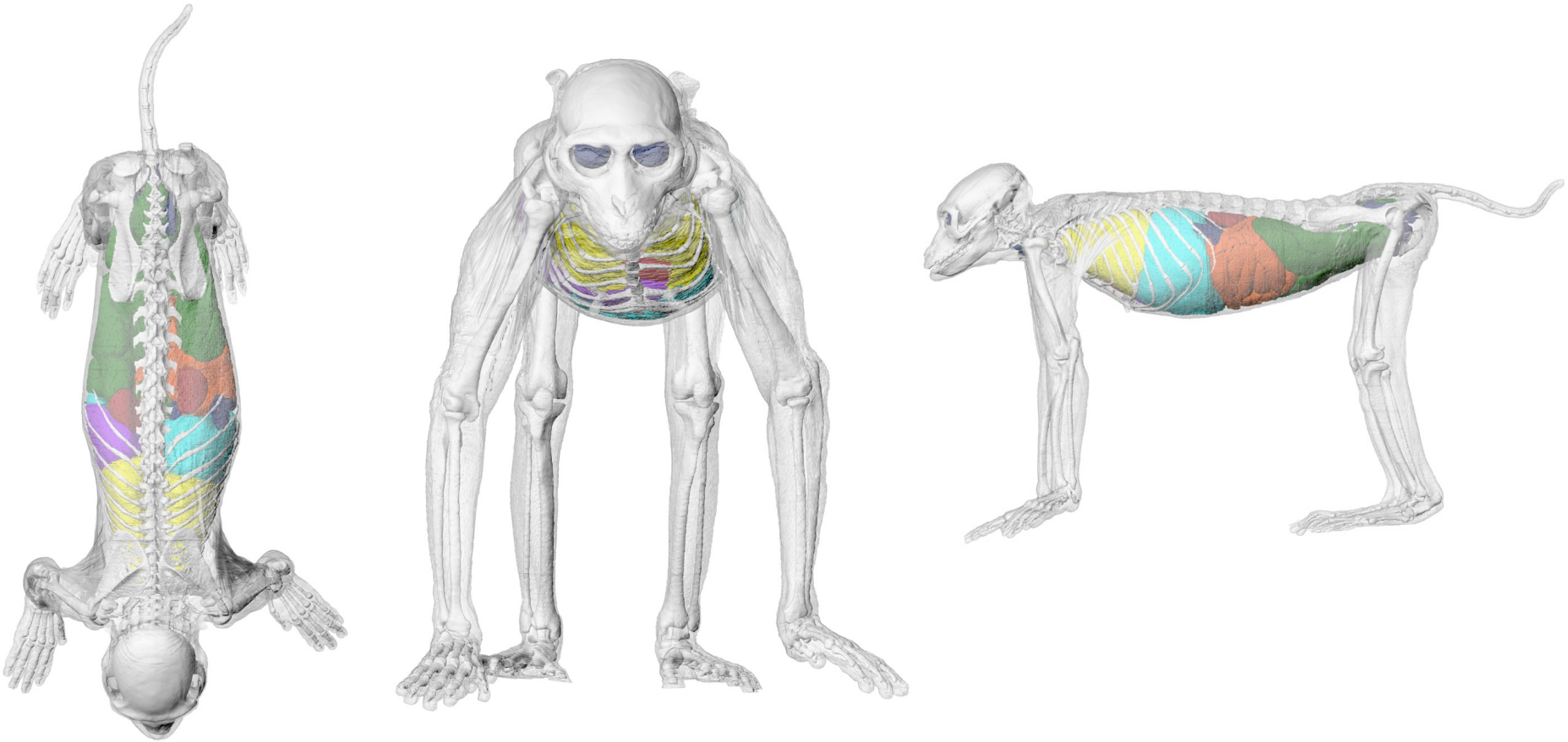

Figure 2. (a) Top, (b) frontal, and (c) left lateral views of the monkey model in crawling posture.

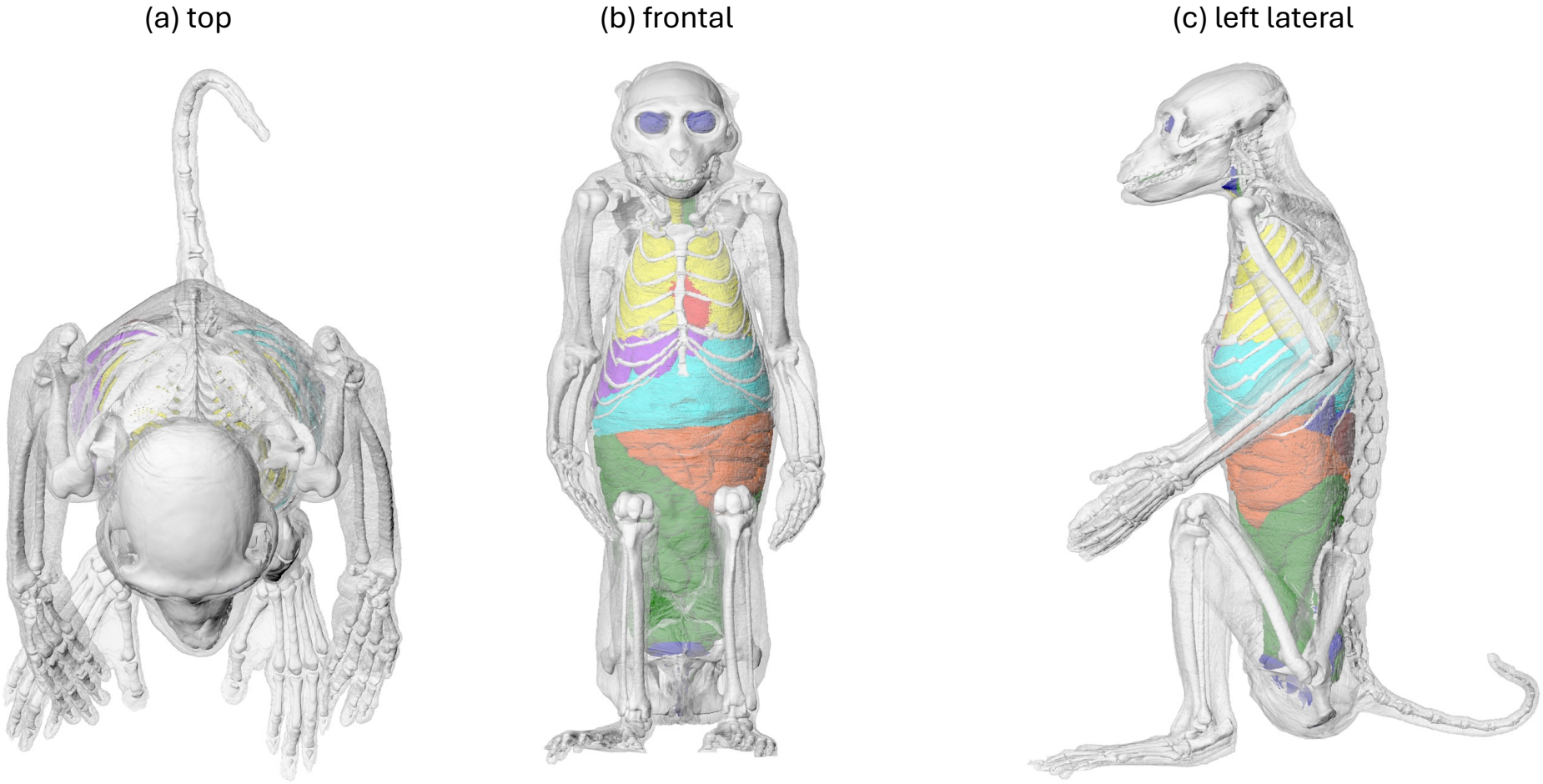

Figure 3. (a) Top, (b) frontal, and (c) left lateral views of the monkey model in squatting posture.

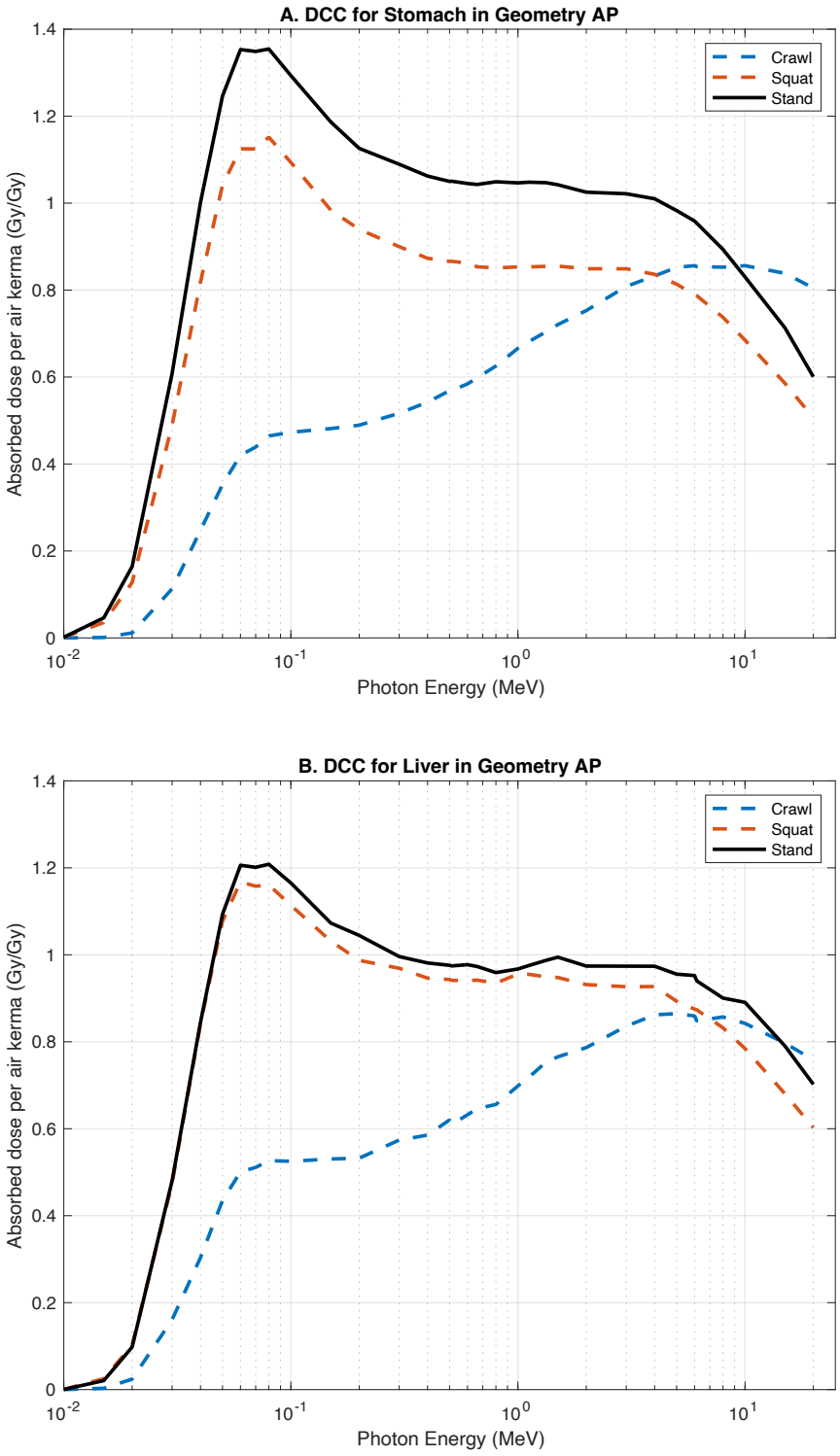

Figure 4. Dose conversion coefficients for (a) stomach, (b) liver, (c) large intestine, (d) lung for the monkey model in crawling, squatting, and standing postures in antero-posterior (AP) irradiation geometry.

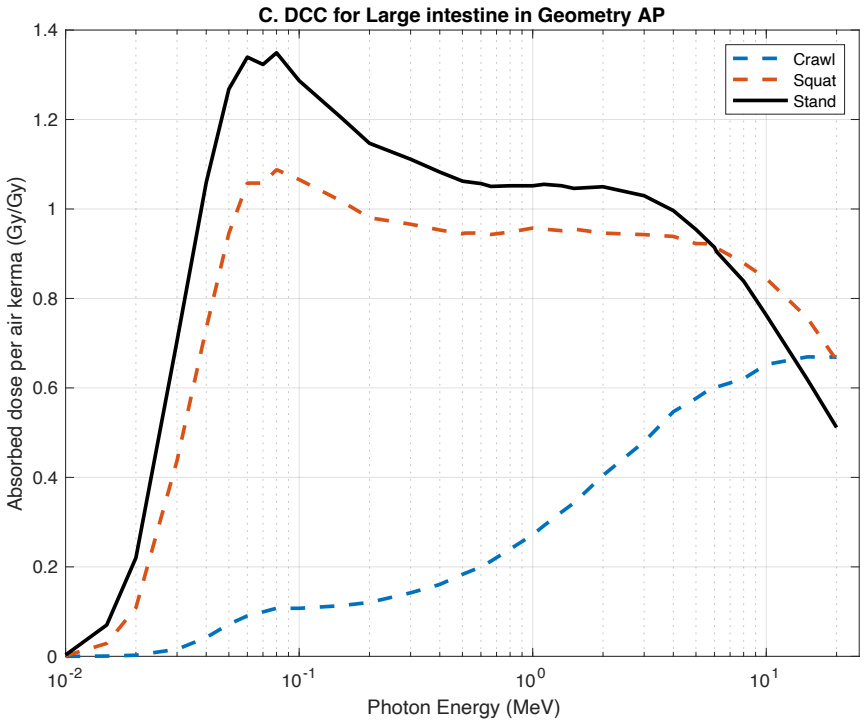

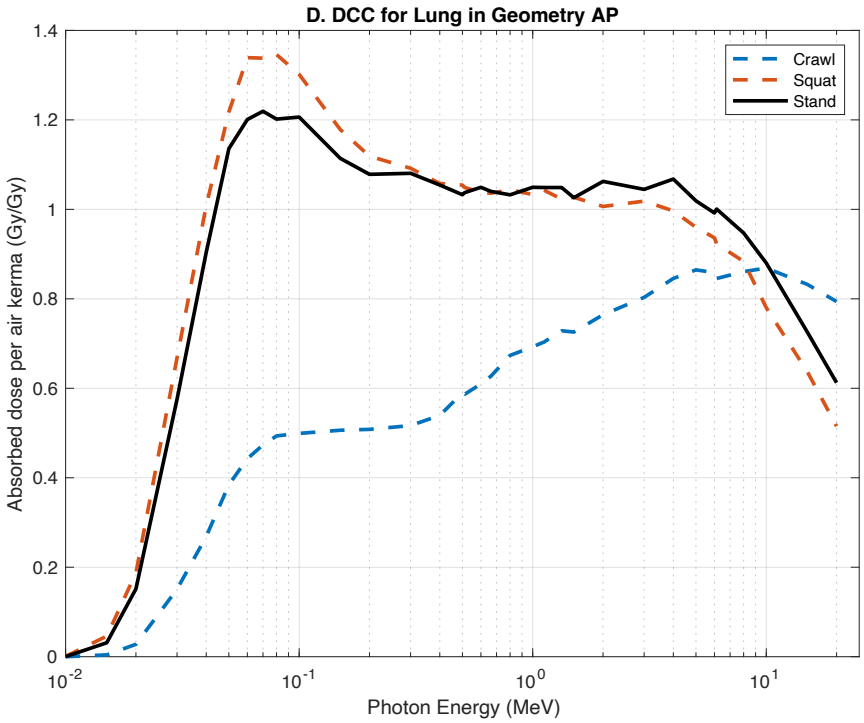

Figure 4. Dose conversion coefficients for (a) stomach, (b) liver, (c) large intestine, (d) lung for the monkey model in crawling, squatting, and standing postures in antero-posterior (AP) irradiation geometry.

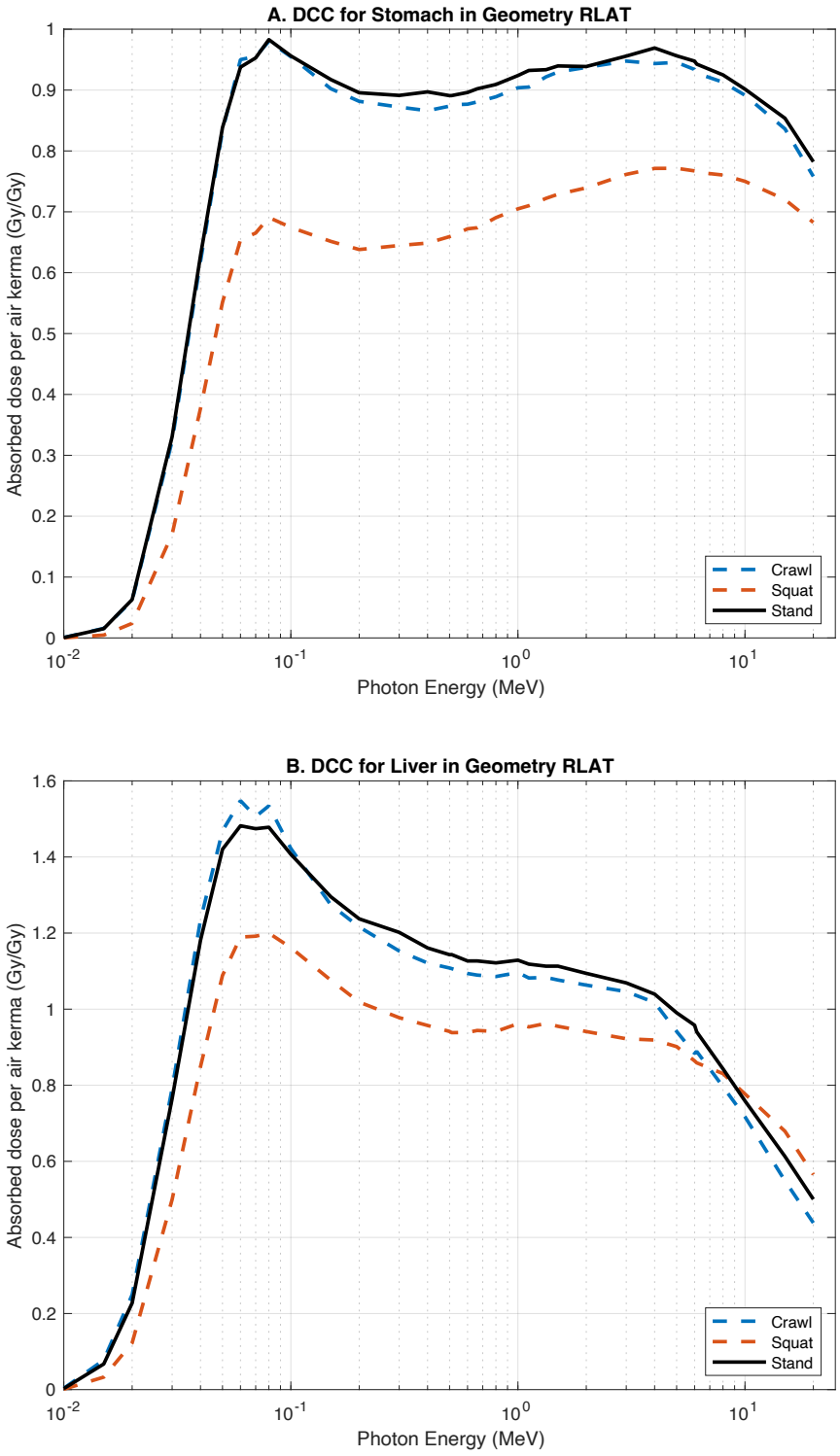

Figure 5. Dose conversion coefficients for (a) stomach, (b) liver, (c) large intestine, (d) lung for the monkey model in crawling, squatting, and standing postures in right lateral (RLAT) irradiation geometry.

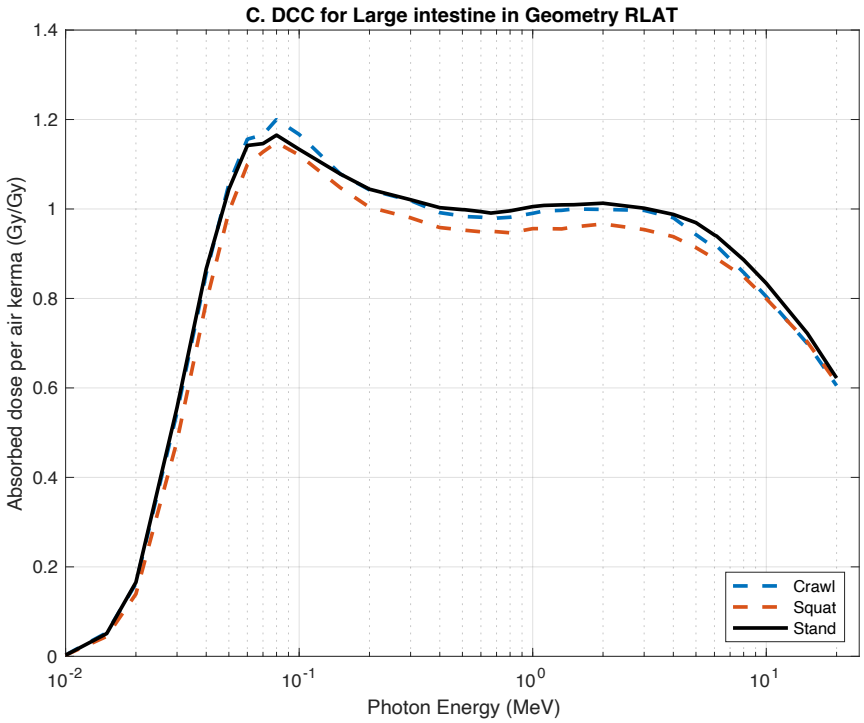

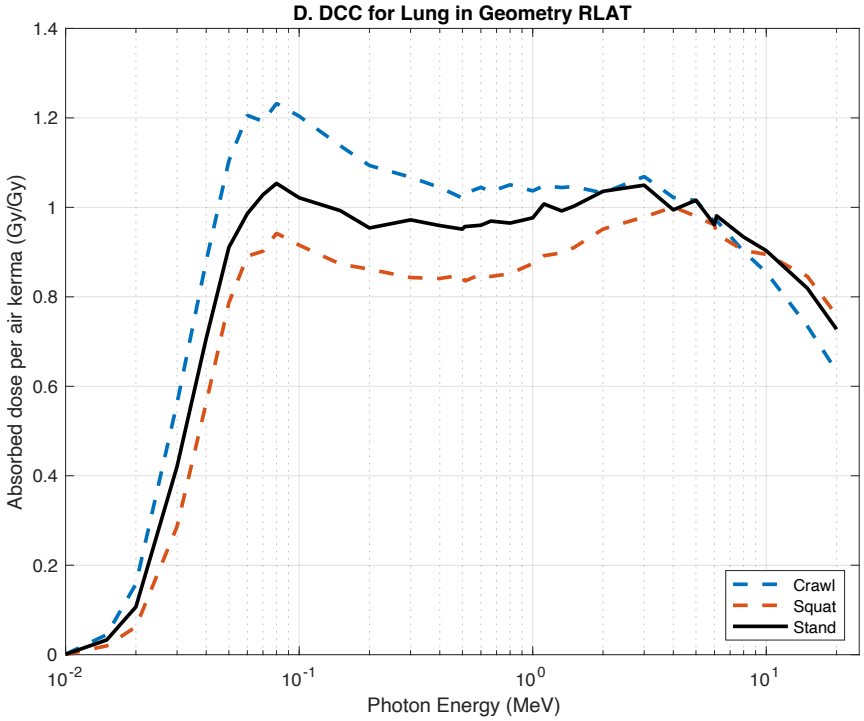

Figure 5. Dose conversion coefficients for (a) stomach, (b) liver, (c) large intestine, (d) lung for the monkey model in crawling, squatting, and standing postures in right lateral (RLAT) irradiation geometry.

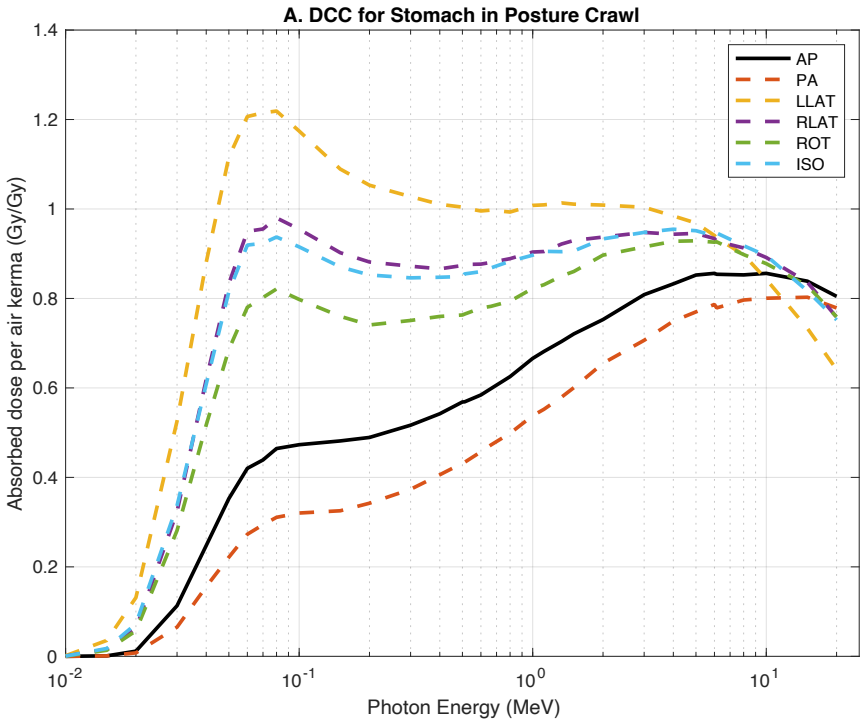

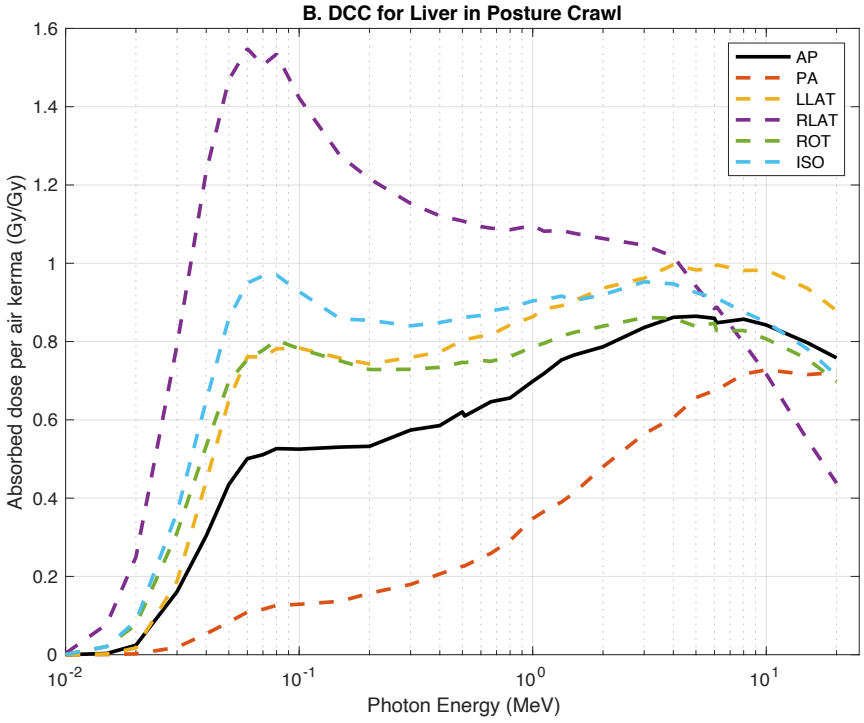

Figure 6. Dose conversion coefficients for (a) stomach, (b) liver, (c) large intestine, (d) lung of the monkey model in **crawling posture** in six irradiation geometries: antero-posterior (AP), postero-anterior (PA), right lateral (RLAT), left lateral (LLAT), rotational (ROT), and isotropic (ISO).

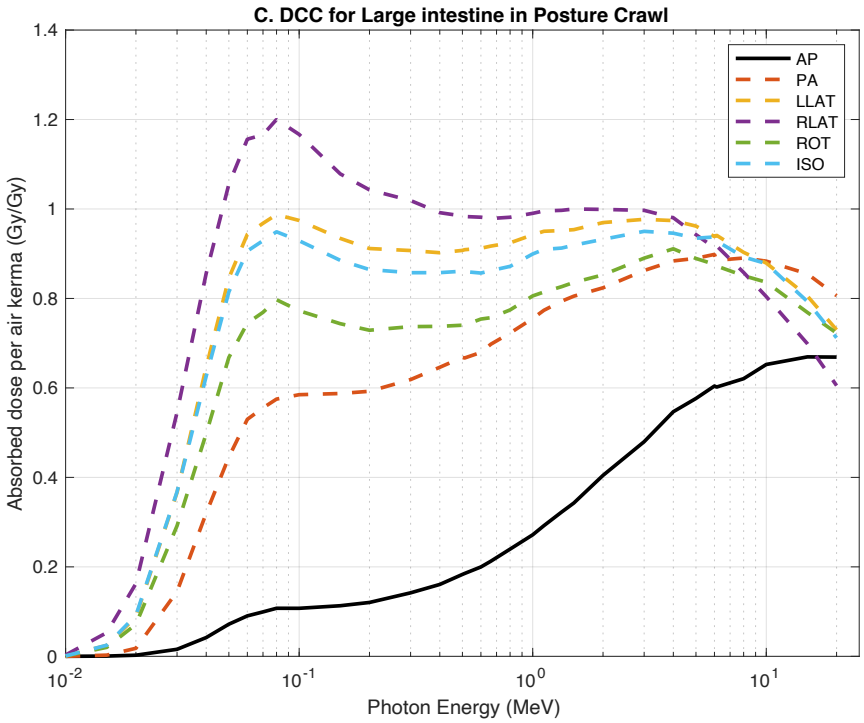

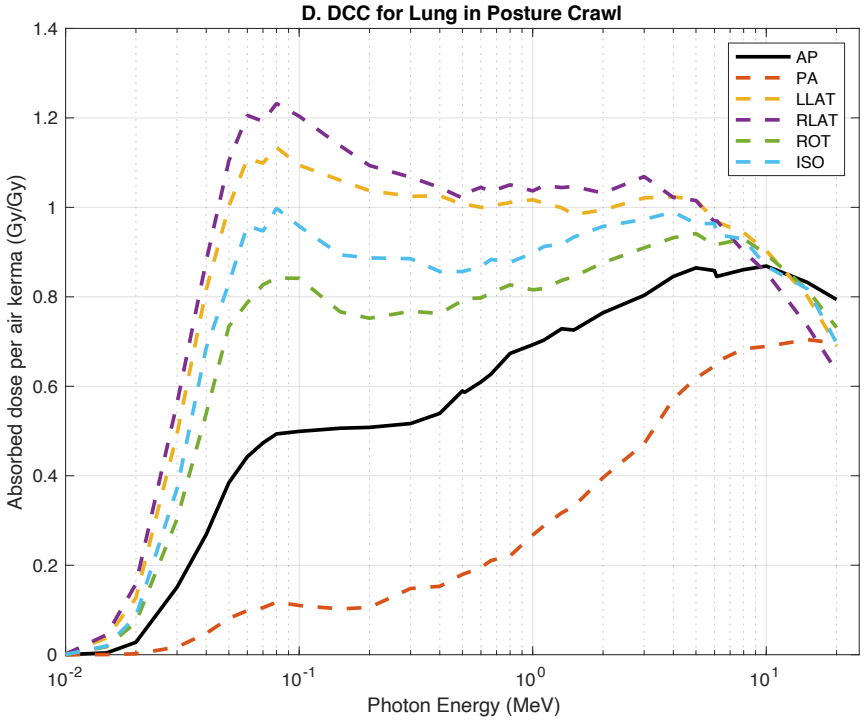

Figure 6. Dose conversion coefficients for (a) stomach, (b) liver, (c) large intestine, (d) lung of the monkey model in **crawling posture** in six irradiation geometries: antero-posterior (AP), postero-anterior (PA), right lateral (RLAT), left lateral (LLAT), rotational (ROT), and isotropic (ISO).

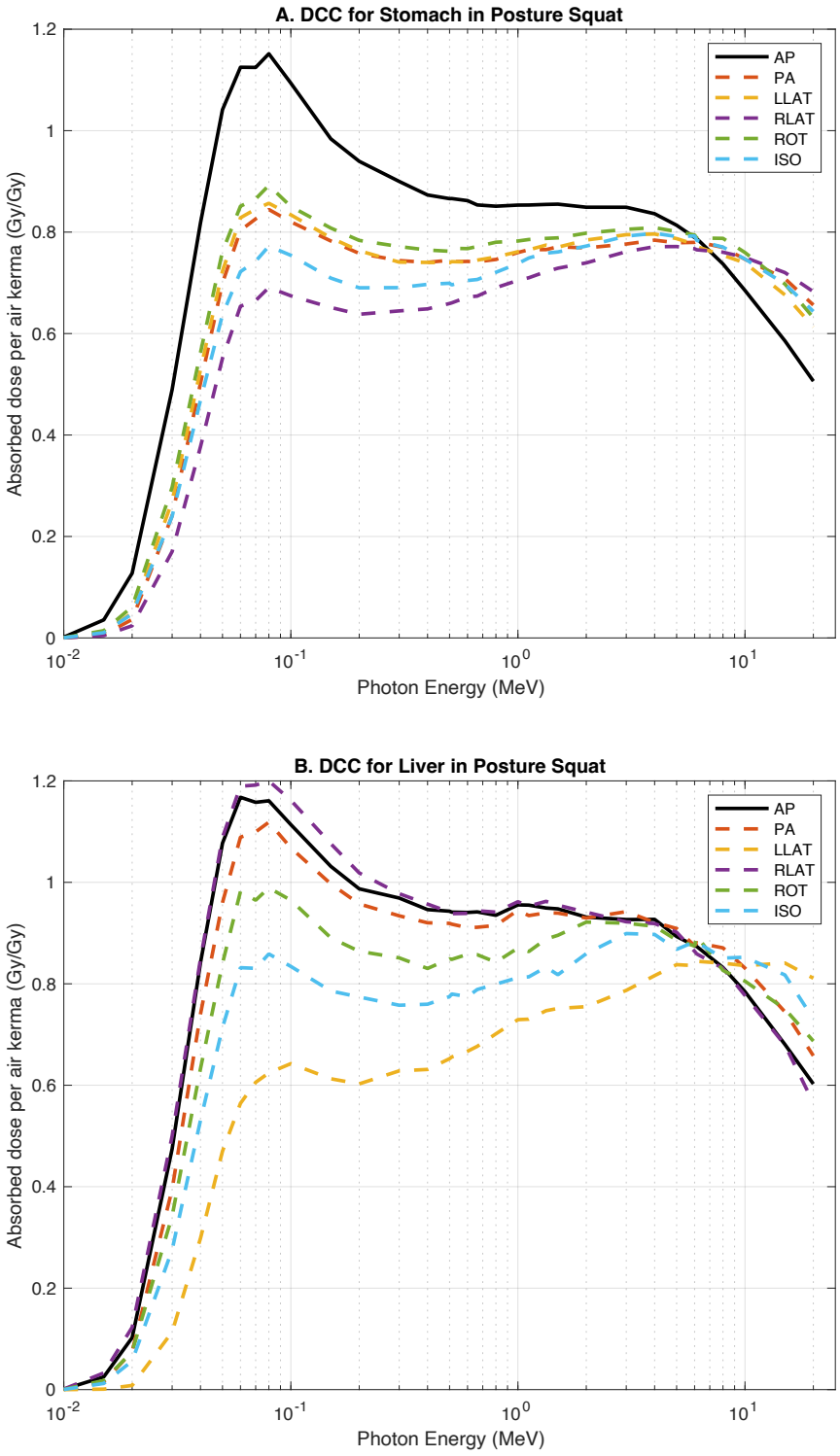

Figure 7. Dose conversion coefficients for (a) stomach, (b) liver, (c) large intestine, (d) lung of the monkey model in **squatting posture** in six irradiation geometries: antero-posterior (AP), postero-anterior (PA), right lateral (RLAT), left lateral (LLAT), rotational (ROT), and isotropic (ISO).

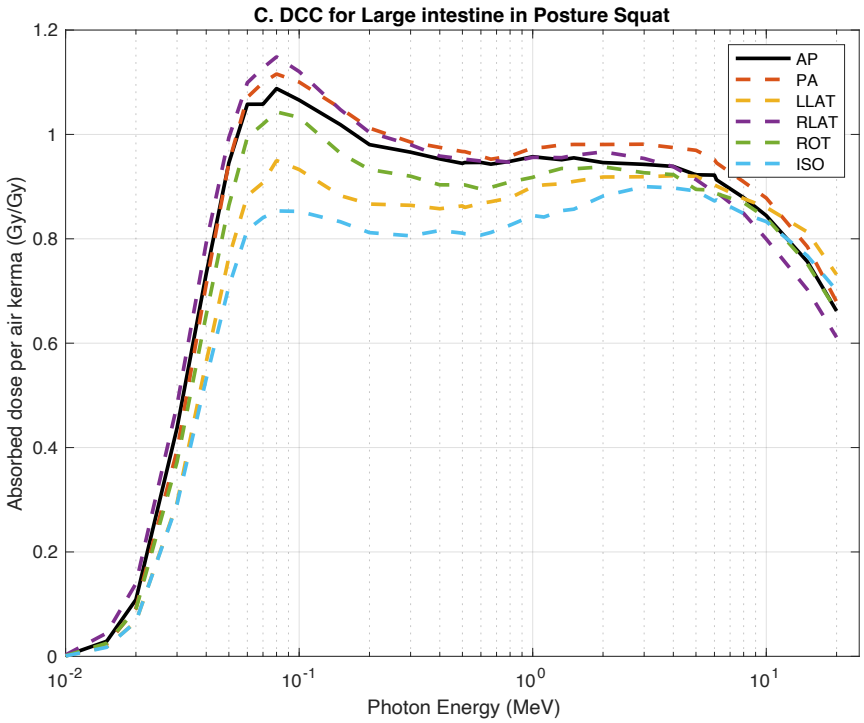

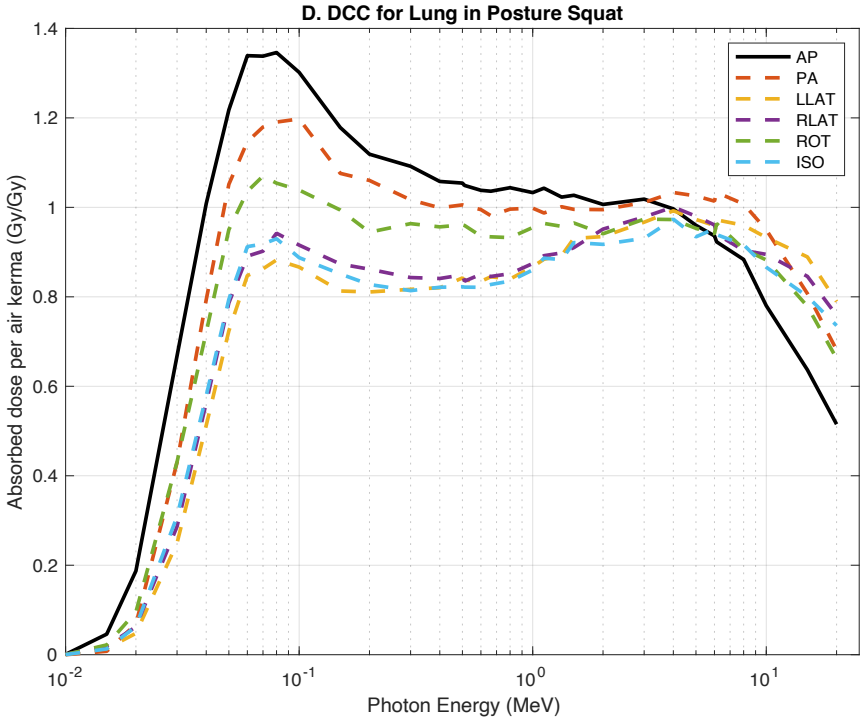

Figure 7. Dose conversion coefficients for (a) stomach, (b) liver, (c) large intestine, (d) lung of the monkey model in **squatting posture** in six irradiation geometries: antero-posterior (AP), postero-anterior (PA), right lateral (RLAT), left lateral (LLAT), rotational (ROT), and isotropic (ISO).

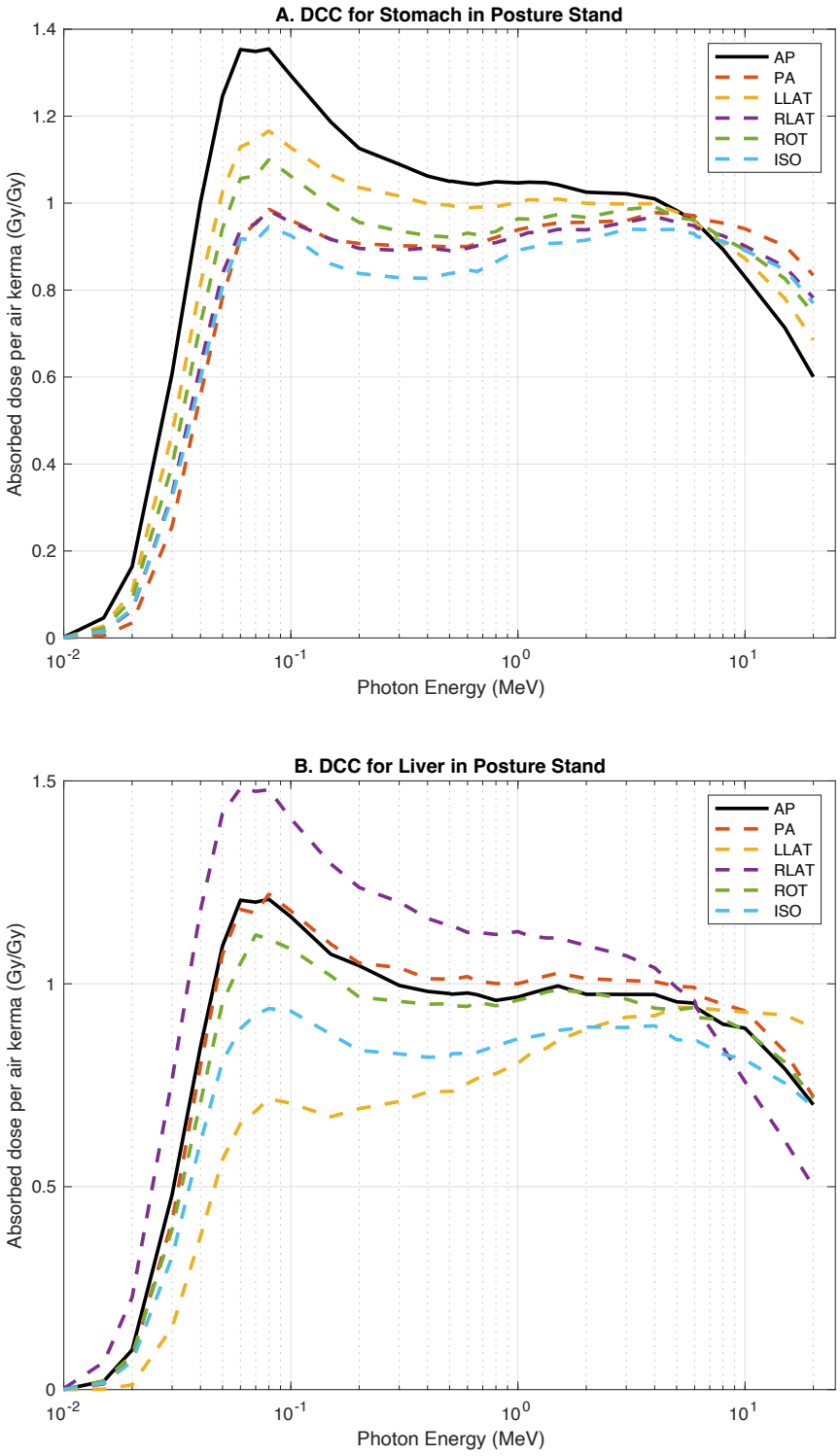

Figure 8. Dose conversion coefficients for (a) stomach, (b) liver, (c) large intestine, (d) lung of the monkey model in **standing posture** in six irradiation geometries: antero-posterior (AP), postero-anterior (PA), right lateral (RLAT), left lateral (LLAT), rotational (ROT), and isotropic (ISO).

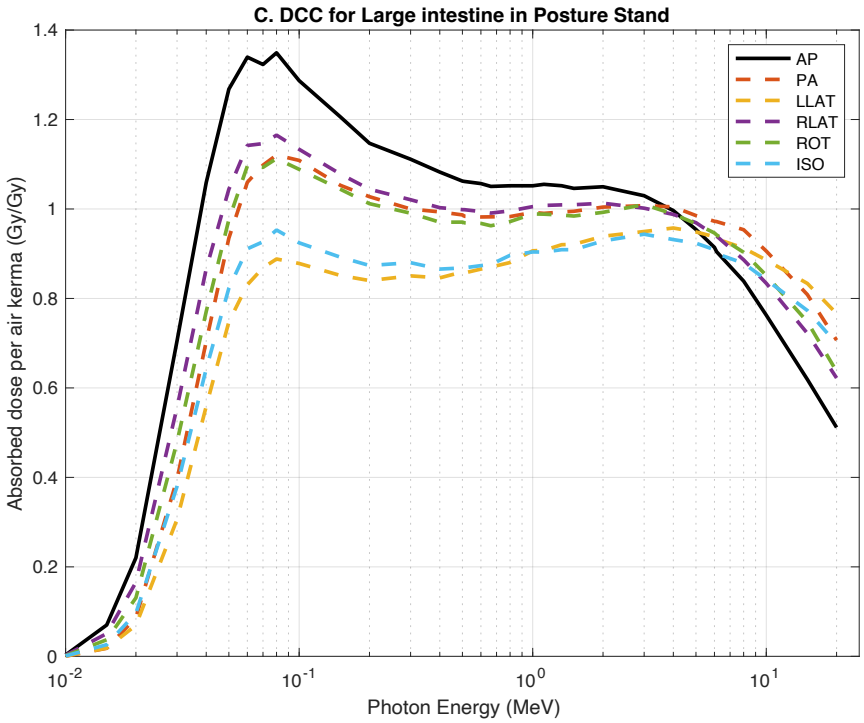

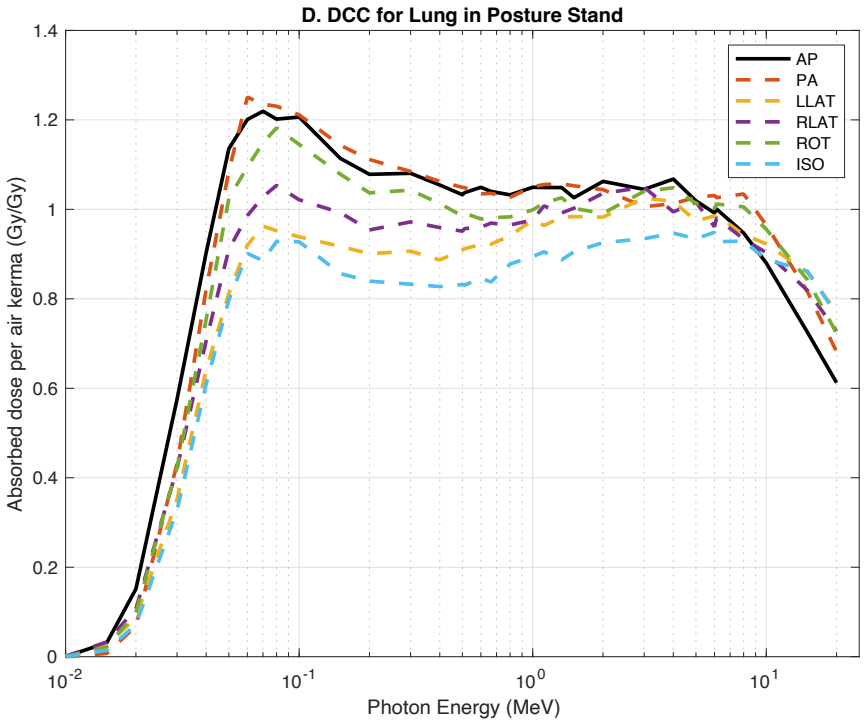

Figure 8. Dose conversion coefficients for (a) stomach, (b) liver, (c) large intestine, (d) lung of the monkey model in **standing posture** in six irradiation geometries: antero-posterior (AP), postero-anterior (PA), right lateral (RLAT), left lateral (LLAT), rotational (ROT), and isotropic (ISO).

Table 1. Organs and tissues of the monkey anatomy model by system for which radiation dose was calculated using Monte Carlo radiation transport methods.

Systems	Organs and Tissues
Digestive	Tongue, esophagus, stomach, liver, small intestine, large intestine, and gall bladder
Lymphatic	Spleen
Endocrine	Thyroid gland, adrenal gland
Integumentary	Skin
Muscular	Muscle
Cardiovascular	Heart
Productive	Ovary, uterus
Urinary	Kidney, urinary bladder
Respiratory	Lung, trachea, bronchus
Nervous	Dura mater, cerebrospinal fluid, frontal lobe, occipital lobe, parietal lobe, temporal lobe, white matter, hippocampus, hypothalamus, thalamus, cingulate gyrus, cerebellum, midbrain, pons, medulla oblongata, spinal cord
Visual	Vitreous humor, lens cortex and nucleus, lens nucleus